

# On D0 brane polarization by tidal forces

Vatche Sahakian<sup>1</sup>

*Laboratory of Nuclear Studies  
Cornell University  
Ithaca, NY 14853, USA*

## Abstract

Gravitational tidal forces may induce polarization of D0 branes, in analogy to the same effects arising in the context of constant background gauge fields. Such phenomena can teach us about the correspondence between smooth curved spacetime and its underlying non-commutative structure. However, unlike polarization by gauge fields, the gravitational counterpart involves concerns regarding the classical stability of the corresponding polarized states. In this work, we study this issue with respect to the solutions presented in hep-th/0010237 and find that they are classically unstable. The instability however appears with intricate features with all but a few decay channels being lifted. Through a detailed analysis, we then argue that these polarized states may be expected to be long-lived in a regime where the string coupling is small and the number of D0 branes is large.

---

<sup>1</sup>vvs@mail.lns.cornell.edu

# 1 Introduction

Non-perturbative dynamics in string theory leads one to believe that spacetime, when probed near the Planck scale, is to acquire exotic structure; one that appears to involve non-commutativity of coordinates and an associated foam-like picture for space. The focus of most recent programs has been to understand phenomena of non-commutativity of space-time coordinates as induced by certain supergravity gauge fields in the background of flat space [1]-[13]. These situations present excellent laboratories to test one's intuition with respect to non-commutative geometry, decoupled from gravitational complications. We still however lack a fundamental understanding correlating notions of smoothly curved spacetime, as it arises in the context of familiar gravitational dynamics, and the underlying Planck scale fuzziness (for recent work addressing this question, see [14, 13]).

In a previous work [15], we attempted to address this issue by trying to understand how information about curved spaces, organized for example in derivatives of the metric at a given point, can get encoded into D brane coordinates; given that D branes are known to be natural probes of short length scales. We focused on D0 branes immersed in curved spaces, and used the results of [16, 14, 7, 17, 18, 10, 11, 19] to explore the resulting dynamics through the non-abelian Dirac-Born-Infeld (DBI) action. We identified extrema of this action corresponding to polarized D0 branes; polarization being induced by gravitational tidal forces. From this setting, we learned about the balance of forces between the smooth gravitational background fields and the inter-brane interactions described through non-commuting matrices. And we found a map between data about the smooth background geometry and the structure constants of algebras that characterize the D0 brane matrix coordinates.

An issue of concern in this picture is the classical stability of the polarized configurations. In the scenario of interest, the system is described by a bottomless potential, with directions corresponding to diagonal matrices that can lower the energy indefinitely. Physically, these directions correspond to channels for evaporation into D0 branes that do not have any collective coherence. The question is then whether the extrema of [15] are local minima of the potential energy; hence, corresponding to metastable configurations; or whether they are classically unstable states and would decay promptly into D0 brane gas.

The purpose of the current work is to address this issue of stability. We will find that the relevant extrema of the DBI action are saddle points of the potential energy, and are hence classically unstable. The instability is of a peculiar nature, with most directions in phase space leading to stable modes; including diagonal matrix channels. Using this information, we then estimate the time the system spends near these extrema and argue that, for large number of D0 branes, and small enough string coupling, this timescale can be very long; that is long enough to make the polarized states physically relevant to the dynamics of the system. The basic idea is that small string coupling increases the inertia of the D0 branes;

and that the available phase space leading to decay, as a fraction of the total phase space, decreases in volume as  $1/N^2$  for one particular class of polarized states.

In Section 2, we briefly review the problem at hand. In Sections 3 and 4, we present the spectrum of the oscillators resulting from perturbing the solutions of concern. In Sections 5 and 6, we analyze the dynamics of decay, present the main conclusions of this work, and assess the relevance of the discussion to understanding non-commutativity in curved spaces. Finally, Section 7 contains some of the details of the calculations.

## 2 Preliminaries

We consider a static field configuration of type IIA supergravity involving non-trivial metric, dilaton and RR two-form field strength; all other fields being assumed zero. A collection of  $N$  D0 branes is to propagate in this space as a probe of the geometry. We concentrate on a regime where back-reaction effects and radiation from the accelerating D0 branes can be ignored. The dynamics may be described by the non-Abelian 0 + 1 dimensional DBI action with gauge group  $U(N)$ . Expanding this action to quadratic order in  $\alpha'$ , we can separate the center of mass motion of the D0 branes from the remaining dynamics in the  $SU(N)$ . This  $U(1)$  sector then describes the collective motion of the D0 branes as they fall along a geodesic trajectory in the given background geometry (see [15] for the details). Choosing Fermi normal coordinates [21], we focus on the  $SU(N)$  dynamics as seen by an observer falling with the center of mass of the D0 branes. We look for solutions in  $SU(N)$  describing D0 branes polarized into D2 branes under the influence of tidal-like forces that pull apart the configuration. The energy is given by

$$E = \frac{(2\pi l_{str}^2)^2}{g_{str} l_{str}} \text{STr} \left\{ \frac{1}{2} \dot{\Phi}^n \dot{\Phi}^n + M_{nm} \Phi^n \Phi^m - \frac{1}{4} [\Phi^n, \Phi^m] [\Phi^n, \Phi^m] \right\} , \quad (1)$$

where

$$M_{nm} \equiv -\frac{1}{4} G_{00, nm} - \frac{1}{2} C_{0, nm}^{(1)} . \quad (2)$$

$C^{(1)}$  is the one form RR potential, and the time-time component of the metric  $G_{00}$  is given with respect to the string frame metric as

$$G_{00} = e^{-2\phi} G_{00}^{str} . \quad (3)$$

The  $\Phi^n$ 's are time-dependent traceless Hermitian matrices, with  $n = 1, \dots, 9$ . The equation of motion is

$$\ddot{\Phi}^n + 2M_{nm} \dot{\Phi}^m + [\Phi^m, [\Phi^m, \Phi^n]] = 0 . \quad (4)$$

We specialize to a background geometry of the form

$$M_{ij} = \delta_{ij}M , \quad M_{ab} = \delta_{ab}M' \quad \text{with} \quad M < 0 . \quad (5)$$

Here,  $i, j = 1, 2, 3$  and  $a, b = 4, \dots, 9$ ; the nine dimensional space is hence split into two subspaces. For scenarios involving somewhat more general backgrounds, the reader is referred to [15]. With the present choice, we are focusing on configurations that can potentially carry D2 brane charge; the D2 branes extending in the three directions labeled by  $i, j$ . And the isotropy of the background within each subspace is chosen to avoid unnecessary clutter; the general conclusions we will reach are expected to be insensitive to anisotropy. The condition  $M < 0$  implies that the tidal forces are pulling apart the D0 branes, as opposed to exerting an inward pressure.

There are several classes of solutions to (4). A dynamical scenario is realized by choosing the  $\Phi^n$  matrices in the Cartan subalgebra of  $SU(N)$ ; *i.e.* diagonal traceless matrices. With  $M < 0$ , this describes the D0 branes evaporating to infinity, without any collective coherence. This is an uninteresting scenario that appears to be the preferred channel for the evolution of the system.

A closer inspection of equation (4) leads to other solutions that describe polarized configurations; perhaps metastable states that the system may prefer given the appropriate initial conditions. One such realization describes a time-independent non-commutative sphere [15]

$$\Phi^i = \pm \frac{\sqrt{-M}}{2} \tau^i , \quad \Phi^a = 0 , \quad (6)$$

which couples to the D2 brane three-form potential. The  $\tau^i$ 's are the  $SU(2)$  Pauli matrices in an  $n \times n$  representation embedded in  $N$  dimensional  $SU(N)$  matrices (with  $n \leq N$ ); with our choice of normalization, the algebra is

$$[\tau^i, \tau^j] = 2 i \varepsilon_{ijk} \tau^k . \quad (7)$$

This D2 brane extends in the three dimensional isotropic subspace of the nine dimensional space, and has size [22, 15]

$$\frac{r}{2\pi\alpha'} = \left(-\frac{3M}{4}\right)^{1/2} (n^2 - 1)^{1/2} . \quad (8)$$

Consistency of our approach requires that this size be much smaller than the length scale set by the background field  $M$ ; so that, locally, the geometry is almost flat. This statement interestingly can be written as a bound on  $n$

$$n \ll \frac{1}{M\alpha'} \equiv \mathcal{A} , \quad (9)$$

where  $\mathcal{A}$  can be thought of as a measure of area constructed from the local curvature scale in Planck units. We will refer to the  $n = N$  case as the maximal non-commutative sphere.

Furthermore, the situation we consider necessarily involves a “slow” evolution of the center of mass of the D0 branes in the background geometry. It is well known that the Fermi normal coordinates are a good approximation of the local structure of space when time derivatives of the metric are much smaller than space derivatives [21]. This may for example be achieved by a judicious choice of initial conditions. Crudely speaking, we need to focus on parts of the history of the configuration where the system moves at small “speeds”  $L/T$ ; where  $L$  is the local length scale set by  $M \sim 1/L^2$ , and  $T$  is the typical proper-time scale over which  $M$  evolves. As the D0 branes will see the fields about them vary slowly in this sense, static solutions like (6) may be considered, and the adiabatic evolution of the non-commutative sphere is described (up to issues regarding its stability that we will address later) by introducing the time dependence through the background field  $M \rightarrow M(t)$  in (6). Naturally, when we refer to a configuration as being long-lived or metastable, we imply that its lifetime is of order  $T$ , not  $L$ . A system that lives for timescales of order  $L$  is short-lived; it would consist of a momentary nucleation in the history of the evolution of the center of mass. The hierarchy between the scales  $L$  and  $T$  will play a crucial role in our analysis of the stability of the solution (6).

The energy of this spherical D2 brane is

$$V_{\text{sph}} = -\frac{(2\pi l_{\text{str}}^2)^2}{8g_{\text{str}}l_{\text{str}}} n(n^2 - 1) M^2 ; \quad (10)$$

while zero energy corresponds to the configuration where all the D0 branes are sitting on top of each other at the origin of the coordinate system. Hence, lowest energy in this set of solutions is achieved when  $n = N$ . We may also view the system from the point of view of the D2 brane world-volume theory; the latter is characterized by a scale of non-commutativity  $\sqrt{\theta} \sim l_{\text{str}}^2/L$ , and an IR cutoff  $\Sigma \sim r$ .

It will be instructive to consider yet another class of static solutions to (4). In particular, we can easily write down the alternative configurations

$$\Phi^1 = 0 , \quad \Phi^2 = \pm \sqrt{\frac{-M}{2}} \tau^2 , \quad \Phi^3 = \pm \sqrt{\frac{-M}{2}} \tau^3 , \quad \Phi^a = 0 ; \quad (11)$$

with all permutations of the signs and of the Pauli matrices being other possible realizations. We will call these non-commutative D2 brane discs; this nomenclature is to be regarded somewhat arbitrary. The energy of these configurations is

$$V_{\text{disc}} = -\frac{(2\pi l_{\text{str}}^2)^2}{6g_{\text{str}}l_{\text{str}}} n(n^2 - 1) M^2 , \quad (12)$$

which is lower than (10) for fixed  $n$ . Issues of classical stability regarding the non-commutative disc and sphere will be addressed in the next section.

### 3 The spectrum of perturbation modes

We first focus on the non-commutative sphere configuration. We perturb the solution by a general traceless Hermitian matrix  $\mathbf{e}^n$

$$\begin{aligned}\Phi^i &= \frac{\sqrt{-M}}{2}\tau^i + \mathbf{e}^i, \\ \Phi^a &= \mathbf{e}^a.\end{aligned}\tag{13}$$

And we study the spectrum of the  $N^2 - 1$  eigenvalues of the equations of motion linearized in  $\mathbf{e}$ . Some of the details of this analysis are presented in Section 7. In this section, we discuss the results.

The equations for  $\mathbf{e}^a$  decouple from those for  $\mathbf{e}^i$ . Requiring that the  $\mathbf{e}^a$  modes are oscillatory leads to the statement

$$M' \geq M.\tag{14}$$

Note that  $M < 0$ . Negative values for  $M$  or  $M'$  correspond to tidal forces pulling the D0 branes away from the origin in the relevant directions of space. When the bound (14) is satisfied, there are no instabilities in the six directions transverse to the D2 brane; tachyonic modes would appear only when  $M'$  becomes negative *and* is of the same order as  $M$ . To sustain a D2 brane configuration expanding in the three dimensional subspace, it was found in [15] that the negative tidal forces in the three different directions that we labeled by  $i, j$  needed to be of comparative magnitudes. We then see in (14) the corresponding statement with respect to the other six space dimensions. When the inequality (14) fails, we may then expect polarization of the D0 branes into D8 branes instead. If we were to consider the case with anisotropic six dimensional subspace, we would expect to realize non-commutative D4 and D6 branes.

The dynamics of the  $\mathbf{e}^i$  modes is considerably richer. We have analyzed the spectrum of eigenvalues in detail first numerically, then identified the analytical pattern underlying it; we present the results with the help of a series of figures.

Figure 1 demonstrates how the number of unstable modes decreases as we increase the size  $n$  of the representation,  $N$  being fixed. All modes are physical, as we have modded out the spectrum with the gauge symmetry of the theory.

In Figure 2, we focus on the maximal representation  $n = N$  and vary  $N$ . The zero modes include gauge transformations; the number of physical zero modes is always seven. A striking

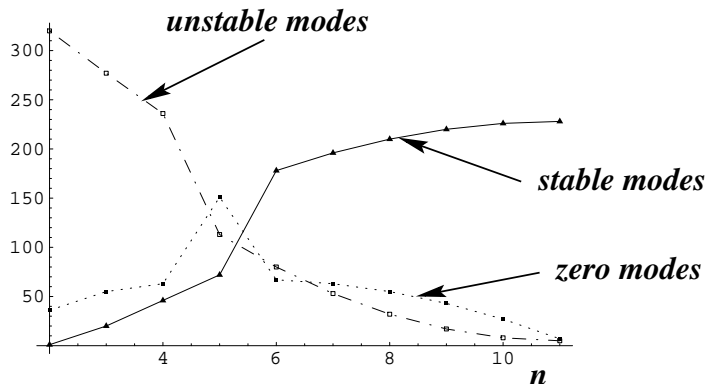


Figure 1: *Spectrum of eigenvalues for the non-commutative sphere: we plot  $n$  on the horizontal axis, and count number of eigenvalues on the vertical.  $N$  is fixed to 11, while  $n$ , the representation size of the  $SU(2)$  embedded in  $SU(N)$ , is being varied from 2 to 11. We have also subtracted from the number of zero modes the dimension of the space of gauge transformations  $n^2 - 1$ .*

feature is that the number of tachyonic modes is also constant; unstable modes are five in number for all  $N$ . The rest of the perturbations correspond to stable modes. In particular,  $3N - 5$  of the Cartan directions are lifted. We will appreciate more this phenomenon when we look at the disc solutions along the same ideas.

It is well-known that the space of  $N \times N$  traceless Hermitian matrices can be organized into the spherical harmonic modes of  $SU(2)$  [23, 22]. For a given  $N$ , one needs angular momentum modes  $l = 1, 2, \dots, N - 1$ ; with  $\sum_{l=1}^{N-1} (2l + 1) = N^2 - 1$ . We will use this basis for the matrices  $\mathbf{e}^n$  and label the resulting eigenvalue spectrum by the harmonic modes they are associated with.

We find that the five unstable modes of the non-commutative sphere solution have mode number one. They are longest wavelength perturbations and lie in an  $SU(2)$  subalgebra of  $SU(N)$ , with eigenvectors given by

$$\begin{aligned}
 \mathbf{e}^1 &\rightarrow \tau^1 \left| \begin{array}{c|c|c} 0 & \tau^2 & 0 \\ \tau^2 & \tau^1 & \tau^3 \\ -\tau^3 & 0 & \tau^2 \end{array} \right. \tau^3 \\
 \mathbf{e}^2 &\rightarrow -\tau^2 \left| \begin{array}{c|c|c} 0 & \tau^2 & 0 \\ \tau^2 & \tau^1 & \tau^3 \\ -\tau^3 & 0 & \tau^2 \end{array} \right. 0 \\
 \mathbf{e}^3 &\rightarrow 0 \left| \begin{array}{c|c|c} 0 & \tau^2 & 0 \\ \tau^2 & \tau^1 & \tau^3 \\ -\tau^3 & 0 & \tau^2 \end{array} \right. \tau^1
 \end{aligned} \tag{15}$$

The first two columns correspond to squashing the sphere into a pancake, one in each of three directions; in this respect, only two are linearly independent. The last three modes are “rotations with the wrong sign”<sup>2</sup>. The eigenvalues for all these unstable modes are given by

<sup>2</sup>The three true rotation modes are zero modes, and consist of gauge transformations.

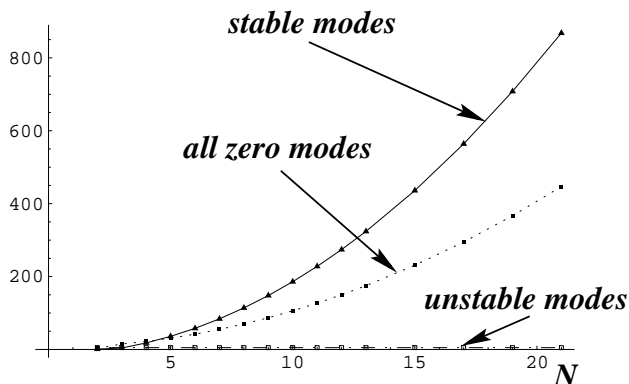


Figure 2: *Eigenvalue spectrum of the maximal non-commutative sphere solution:  $n = N$  is being varied on the horizontal axis, while the number of eigenvalues is plotted on the vertical. The number of zero modes include gauge transformations; the number of physical zero modes is equal to seven for all  $N$ .*

$\omega^2 = 2M$ . The breathing mode,  $\mathbf{e}^i \rightarrow \tau^i$ , which also appears at the longest wavelength, is stable, with frequency  $\omega^2 = -4M$ .

All of the seven physical zero modes are quadrupole moments, with harmonic mode two. Any short wavelength perturbation, shorter than harmonic mode one, is otherwise a stable mode. For example, plucking several D0 branes does not compromise the global coherence of the configuration. All instabilities arise at the longest possible wavelengths, at harmonic mode one. The spectrum of the stable modes is described in Section 7.

Two interesting features of the tachyonic modes for the maximal embedding of  $SU(2)$  into  $SU(N)$  are worth emphasizing: first, that their number is independent of  $N$ ; it is always equal to five; and second, that their masses are independent of  $N$ . One immediate consequence is that the fraction of unstable channels available for decay, out of the  $6(N^2 - 1)$  dimensional phase space available for fluctuations, is parametrically small with large  $N$ . To underscore the peculiarity of this pattern, let us contrast the situation with the other static solutions to (4). First, the  $n$  dimensional representations, with  $n < N$ , have a growing number of unstable modes as a function of increasing  $N$ ; this number grows as  $N^2$ . The masses of these tachyonic modes are all degenerate, scaling as  $\omega^2 = 2M$ . Furthermore, perturbing the disc solution given by (11) in a similar manner, we find the spectrum depicted in Figure 3. The representation here is maximal, with  $n = N$ , and  $N$  is being varied. We see a rise in the number of unstable modes as  $2N - 2$  even for the maximal embedding. Note that these solutions have lower energy than the non-commutative sphere for the same  $N$ ; however, for large  $N$ , we see that they are characterized with a much larger number of decay channels than



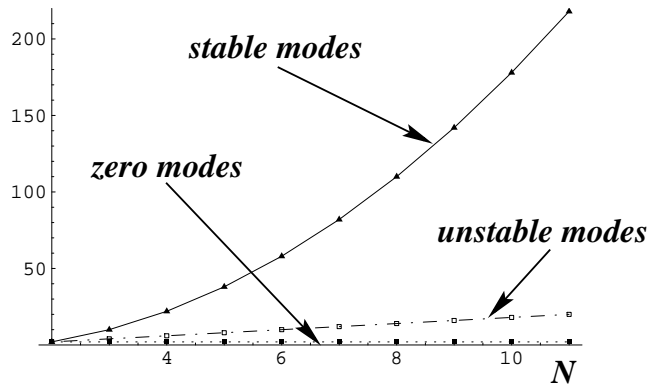


Figure 3: *The non-commutative disc solution: we consider maximal embedding  $n = N$ ;  $N$  is being varied on the horizontal axis. Zero modes include gauge transformations. The number of physical zero modes is fixed to two.*

the maximal sphere. Furthermore, the tachyonic modes are distributed along the spectrum  $\omega^2 = 4M, 6M, \dots, 2NM$ .

We conclude that all of the static solutions presented in the previous Section are classically unstable. All have tachyonic modes, with varying magnitudes and cardinality. The timescale for each decay channel is set by  $L$  (with  $M \sim 1/L^2$ ). As we described above, this is a short time for the objects to be interesting on timescales set by the evolution of the center of mass; the scale we denoted by  $T$ . Our interest lies in tracing the system as it transports itself across many curvature scales in spacetime. However, as we will see in Section 5, a careful analysis leads to the conclusion that, for large  $N$  and small string coupling  $g_{str}$ , the non-commutative sphere solution gets singled out and may be expected to be long-lived.

## 4 The shape of the potential

From our discussion of the spectrum of perturbation modes in the previous section, it is apparent that our static configurations lie at saddle points of the potential. For the maximal non-commutative sphere, the phase space of the perturbations about the solution consists of five unstable tachyonic directions, seven zero modes, and  $2N^2 - 14$  stable channels. In an effort to visualize the landscape of this interesting potential away from its extrema, we plot a couple two dimensional cross-sections. Figure 4 shows three classes of extrema of the potential. In the center, on a bump, is the trivial solution where the D0 branes sit on top of each other, *i.e.*  $\Phi^n = 0$ . The saddle points correspond to the maximal non-commutative sphere solutions. While the local minima appearing at the bottom of paraboloids are the  $n =$

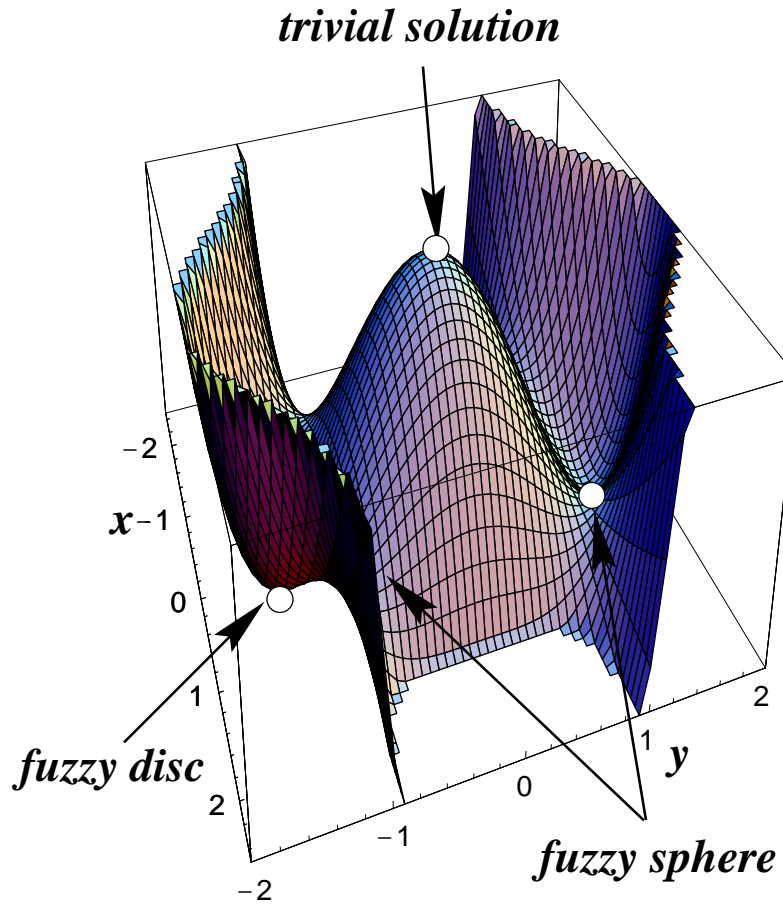


Figure 4: A cross-section of the potential energy in (1): the z-axis is energy, and the cross-section is obtained by  $\Phi^1 = x \Phi_{(0)}^1$ ,  $\Phi^2 = y \Phi_{(0)}^2$ ,  $\Phi^3 = -y \Phi_{(0)}^3$ . We have defined  $\Phi_{(0)}^i \equiv \sqrt{-M\tau^i}/2$ .

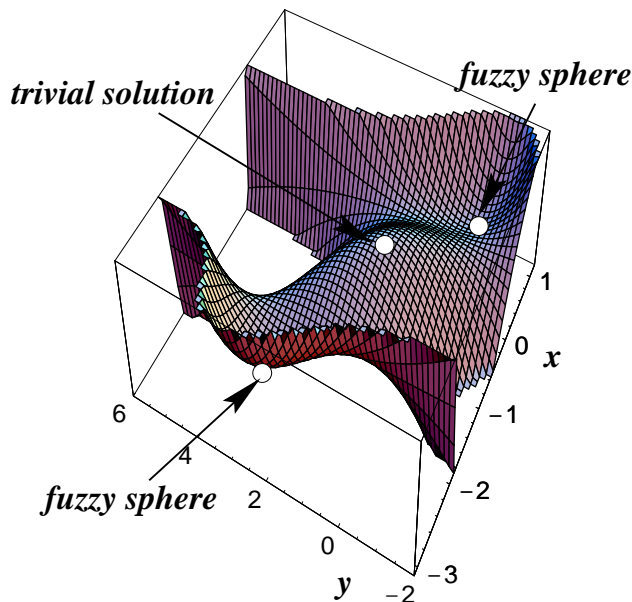


Figure 5: *Another cross-section of the potential energy: this viewpoint is obtained by  $\Phi^1 = \Phi_{(0)}^1 + x \Phi_{(0)}^1$ ,  $\Phi^2 = y \Phi_{(0)}^2 + x \Phi_{(0)}^2$ ,  $\Phi^3 = \Phi_{(0)}^3 + x \Phi_{(0)}^3$ ; with  $\Phi_{(0)}^i \equiv \sqrt{-M\tau^i}/2$ .*

$N$  disc solutions. It is important to emphasize that this is a two dimensional cross section; and the many directions of instability associated with the disc solutions are suppressed. The infinite well appearing in the figure leads to a Cartan direction in  $SU(N)$ ; hence to evaporation into widely separated D0 branes.

Another cross-section of this space is shown in Figure 5. This depicts a more “generic” viewpoint for large  $N$ . The hill in the middle is the trivial solution, while the ditches on its sides correspond to maximal non-commutative sphere solutions. The five unstable directions about the sphere solution do not appear in this cross-section.

These graphical depictions of the energy tell us that the system is a complex one; with many extrema of the potential energy scattered in interesting patterns, in addition to the gorges that lead to evaporation into D0 branes. In the next section, we address questions pertaining to the dynamics of the system in this landscape.

## 5 The timescale of decay

Given that the extrema of the potential energy corresponding to the polarized states are saddle points, the obvious conclusion is that these states, being classically unstable, will

decay; in particular, they would tend to evaporate to widely separated D0 branes. The distribution of these extrema in the landscape of the potential reflects nevertheless certain interesting characteristics of the underlying dynamics; it is information about the balance of forces amongst the D0 branes and background supergravity fields. Furthermore, within the context of the classical instability of these solutions, there remains to determine the role of these states in the dynamics of the system. In particular, we would like to find the likelihood that such polarized states may nucleate; and if they do, to estimate the typical timescales they live, before evaporating into D0 branes. We will see below that there is indeed regimes where these extrema of the potential play a part in the history of the evolution of the D0 branes, as the branes cascade their way down the potential energy.

For the sake of concreteness, we first concentrate on the following scenario. We consider a background field configuration such that, in some region of space, spacetime curvatures are small with respect to the string scale. We project  $N$  D0 branes with some initial velocity from this region into a direction where gradients of background fields become larger. We also arrange our D0 branes into a polarized D2 brane configuration corresponding to the  $n = N$  solution of (6), where  $M$  relates to the initial local curvature scale. The center of mass of the system will follow a geodesic in a rescaled metric [15]; while, in the freely falling frame,  $M$  evolves on timescales of order  $T$ . At every moment in time, we denote the typical length scale over which background fields vary as  $L \sim 1/\sqrt{|M|}$ . The scenario is arranged to be adiabatic, with  $T \gg L$ , at least for the initial part of the trajectory of the center of mass. The eventual outcome is total evaporation into D0 branes; a roll down the bottomless potential. On their way on this ill-fated journey, the D0 branes may however spend a significant amount of time near the initial saddle point or other extrema of the potential energy; that is, wherever timescales of dynamics becomes of order  $T$ . Extrema characterized by times much shorter than this scale, and in particular ones of order  $L$ , will be mostly irrelevant to the overall dynamics of the system. The issue then becomes whether we may encounter basins of “metastability” during this evolution.

Let us try to estimate the time the system will spend in our initial unstable configuration, using the data about perturbation modes we collected in Section 3. Classically, considering the idealized situation whereby the configuration sits initially right on top of the saddle point, with zero initial momentum (in the center of mass frame!), we would immediately conclude that the system stays there forever. However, quantum mechanically, there will be fluctuations in the matrix elements of the coordinates  $\Phi^m$  and their canonical momenta. These new initial conditions will drive the system away from the saddle point, down unstable directions. The evolution of the configuration can be treated classically, except for the input of initial conditions given by the appropriate quantum fluctuations about the saddle point.

We describe the state of the system at some time  $t$  after we let go of it by  $\Phi^n(t)$

$$\Phi^n(t) = \Phi_{(0)}^n + \varepsilon^n(t) , \quad (16)$$

where  $\Phi_{(0)}^n$  is the saddle point solution given by (6) with  $n = N$ , and  $\varepsilon^n(t)$  is the small perturbation evolving the system away from the extremum. To linearized approximation, the dynamics of the  $\varepsilon^n$ 's is that of a collection of decoupled harmonic oscillators, with both real and imaginary frequencies; the latter being the unstable modes. The frequencies of all these oscillators scale as  $1/L$ . Hence, the timescale of the evolution of the system appears to be short. There are several features that may however drive this timescale in the other direction. One is the fact that the number of unstable directions is independent of  $N$ ; another is that the mass of the tachyons is also independent of  $N$ ; and finally, the system is endowed with another dimensionless parameter that sets the scale for the inertia of the configuration. We will argue below that these three ingredients conspire to set a regime where the system can spend significant amounts of time, with respect to scale  $T$ , near certain saddle points, such as the one corresponding to our initial configuration.

We will need to devise a criterion for determining whether the system has moved away from the extremum enough so as to consider it different for the initial object, the non-commutative sphere; regarding it instead a remnant of its decay. A natural approach is to look for fractional changes in gauge invariant observables. For example, we may look at

$$f^2 \equiv \frac{\delta [\text{Tr} (\Phi^n \Phi^n)]}{\text{Tr} (\Phi_{(0)}^n \Phi_{(0)}^n)} . \quad (17)$$

Physically, this is the fractional change in the radius of the non-commutative sphere. We may consider higher moments in  $\Phi^n$  as well; but it will become apparent in the upcoming discussion that they will provide us no stringer probes of the situation.

At this point, the details of the unstable modes will become important. We remind the reader that we have five such modes, all at spherical harmonic mode number one; *i.e.* they are longest wavelength perturbations. The eigenvectors were given in equation (15). All other modes are stable oscillators, or one of seven zero modes. The frequencies of stable oscillations increase parametrically with  $N$ , as described in Section 7. For large times  $t \gg L$ , the relevant dynamics is only the exponential evolution of the unstable modes. Stable and zero modes play a subleading role in estimating (17).

Using (15), we evaluate the fraction (17), keeping only contributions from unstable modes. And we would like this fraction  $f$  to be of order a few percent; this is our choice for a criterion of decay. We note that an important ingredient in computing (17) is the statement that different harmonic modes decouple from each other (see identity (31)). We consequently find that order  $\varepsilon$  contributions to (17) vanish identically because of the particular form of

the unstable eigenvectors and subsequent cancelations<sup>3</sup>. To quadratic order, we easily obtain the leading contribution for large times  $t \gg L$

$$\delta\text{Tr} (\Phi^n \Phi^n) \rightarrow \frac{8}{3} N (N^2 - 1) \varepsilon_u^2(t) . \quad (18)$$

We have assumed comparable initial conditions for all five unstable modes, and we have represented the evolution of these modes with a single function  $\varepsilon_u^2(t)$ . The latter is given by

$$\varepsilon_u(t) = \Delta x \text{ch}(t/L) + L g_{str} l_{str} \Delta p \text{sh}(t/L) . \quad (19)$$

$\Delta x$  and  $\Delta p$  are respectively the fluctuations in position and momentum of a tachyonic mode at the saddle point, used as initial conditions at  $t = 0$  for the classical evolution of the mode. Furthermore, we expect that the initial wavepacket, corresponding to the system sitting at the saddle point with minimal initial momentum, saturates the uncertainty bound  $\Delta p \sim 1/\Delta x$ . Putting things together, we find that for large times  $t \gg L$ ,

$$f \sim \frac{L\Delta x}{l_{str}^2} \left( 1 + \frac{g_{str} l_{str} L}{(\Delta x)^2} \right) e^{t/L} . \quad (20)$$

Note that, despite the fact that the dimension of phase space available for quantum fluctuations is of order  $N^2$ , there is no  $N$  dependence in (20). This is a direct result of the form of the spectrum of eigenvalues discussed in Section 3.

From the work of [24], we know that the expected spread  $\Delta x$  of the wavepacket of each mode is given by the eleven dimensional Planck scale

$$\Delta x \sim l_{pl}^{(11)} \sim g_{str}^{1/3} l_{str} . \quad (21)$$

We then obtain

$$f \sim \frac{Lg_{str}^{1/3}}{l_{str}} \left( 1 + \frac{Lg_{str}^{1/3}}{l_{str}} \right) e^{t/L} . \quad (22)$$

Taking the regime

$$\frac{Lg_{str}^{1/3}}{l_{str}} \ll 1 , \quad (23)$$

we estimate the time  $\tau_0$  the non-commutative sphere spends near this saddle point of the potential energy<sup>4</sup>

$$\tau_0 \sim L \ln \left( \frac{l_{str}}{Lg_{str}^{1/3}} \right) . \quad (24)$$

---

<sup>3</sup>The only contribution to (17) to order  $\varepsilon$  comes from the breathing mode  $\varepsilon^i \sim \tau^i$ , which is a stable oscillator with frequency  $\sim 1/L$ .

<sup>4</sup>The term  $\ln f$  is of order one and can be dropped.

Hence, it is possible for  $\tau_0 \sim T$ , with  $T \gg L$ , if  $g_{str}$  is taken small enough. In such a scenario, as  $L$  evolves on timescales of order  $T$ , the D0 branes would continue to track the initial saddle point. The polarized configuration may then be considered long-lived, disintegrating slowly into incoherent D0 branes.

Repeating our analysis for the case of the disc and non-commutative sphere with  $n < N$ , and using our results for the corresponding eigenvalue spectra given in Section 7, it is easy to see that we get  $\tau \sim (L/\sqrt{N}) \ln(l_{str}/(LN^{1/2}g_{str}^{1/3}))$  and  $\tau \sim L \ln(l_{str}/(LNg_{str}^{1/3}))$  respectively. This arises from the dependence of the number of unstable modes, and the corresponding tachyonic masses, on  $N$ ; for larger  $N$ , there are more channels of decay, with larger masses for the tachyons in units of  $L$ . Without going into the details, it is sufficient to observe that the disc and  $n < N$  spherical solutions will then have parametrically shorter “lifetimes” than (24) for large  $N$ .

This distinguishing property of the  $n = N$  non-commutative sphere solution becomes more important when we want to determine the probability the system will find a “basin” of metastability if it were to start its journey with more generic initial conditions. Noting that the dimension of the Cartan subalgebra scales as  $N$ , while the dimension of the non-abelian channels scales as  $N^2$ , and that the maximal sphere solution is at a minimum in almost all of those directions (including the Cartan ones), we expect that, for larger values of  $N$ , the system would be more likely to find the non-commutative sphere configuration in the phase space available to it. Furthermore, the  $n < N$  and disc solutions become shorter lived in this limit. While the dynamics can be get very complicated, a large  $N$  limit leads to a simplification in this sense.

Focusing on the non-commutative sphere solution with maximal embedding  $n = N$  as the prime candidate for a long-lived polarized configuration, we note however that the scaling in (24) puts the string coupling at a disadvantage in the competition between the various parameters; in particular, a logarithm of  $g_{str}$  is to compensate a power law in  $L/T$ . Hence, the regime we may envisage where the maximal non-commutative sphere solution will play a salient role in the evolution of the system involves a delicate hierarchy between different scales; which we need to discuss carefully both from the point of view of the embedding string theory, as well as that of the quantum mechanics that describes the dynamics of the D0 branes.

Figure 6 depicts all scales in the problem written with respect to IIA string theory and D0 brane quantum mechanics variables. For large  $N$ , the relevant coupling in the 0+1 dimensional Yang-Mills theory is

$$(g_{\text{eff}}(\mu))^2 \equiv \frac{g_Y^2 N}{\mu^3} \equiv \frac{g_{str} N}{(l_{str}\mu)^3}, \quad (25)$$

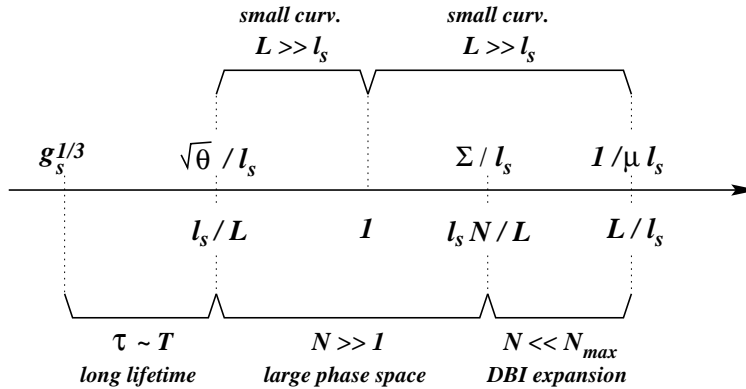


Figure 6: The hierarchy between the various scales of the problem. The axis is labeled by various length scales in string units.  $\sqrt{\theta}$  denotes the “UV cutoff” in the non-commutative worldvolume theory of the D2 brane sphere;  $\Sigma$  is the IR cutoff due to the topology of the configuration; and  $\mu$  is the energy scale at which the effective 0+1 dimensional Yang-Mills coupling is evaluated at in the expression for the lifetime of the non-commutative sphere (26). All brackets indicate a large hierarchy between the corresponding scales; the associated labels indicate the reasons for the needed hierarchies.

where  $\mu$  is the energy scale at which the coupling is measured. We then can write

$$\tau_0 \sim L \ln \left( \frac{N}{(g_{\text{eff}}(1/L))^2} \right). \quad (26)$$

For a perturbative regime in this effective coupling, the lifetime  $\tau_0$  is then pushed toward larger values. Hence, from the quantum mechanics point of view, we need a weakly coupled system, in the large  $N$  limit, so that  $\tau \sim T \gg L$ . Note however that we have an upper bound on  $N$  coming from the requirement that the expansion of the DBI action is self-consistent; this bound is given by (9), or  $N \ll N_{\text{max}} \sim L^2/l_{\text{str}}^2$ . Of course, we also need weak background curvature scales,  $L/l_{\text{str}} \gg 1$ . In type IIA background geometry language, the regime of interest is somewhat similar to the decoupling limit of the 0+1 Yang-Mills theory; *i.e.* we want small coupling  $g_{\text{str}} \rightarrow 0$ , large  $N$ , and the coupling constant of the quantum mechanics held fixed (and small). The summary of all these scales and the relevant bounds is shown in the figure.



## 6 Reflections

It is instructive to push our analysis to the limits of its validity. Looking at (24), we can see that the polarization effect becomes more important when the center of mass is “moving fast”,  $L \sim T$ . The non-commutative state is also longer lived in regions of space with higher curvatures, near stringy length scales  $L \sim l_{str}$ . Even though our description clearly breaks down before these bounds are reached, we may learn from these limits that polarization effects by gravitational tidal forces may be most relevant, for example, near singularities. We may also expect that the coherence of the polarized configuration will get compromised as the center of mass slows down or when entering into regions of spacetime with progressively smaller curvature scales.

In summary, we have argued for a regime where we expect the D0 branes to cascade down the potential energy landscape, with possibly short visits to the various extrema with  $n < N$ , and settling into the  $n = N$  non-commutative sphere configuration for significant amounts of time; finally, the system will find the Cartan directions of commuting matrices, and we are left with a collection of widely separated D0 branes without any collective coherence; which we may regard as the by-product of evaporation of the maximal non-commutative sphere. It is important to emphasize the role of the large  $N$  limit in this picture. The regime of small string coupling increases the inertia of all configurations corresponding to extrema of the potential energy. In this respect, the statement regarding a long lifetime for these classically unstable states is trivial, being relevant for all the polarized configurations. The large  $N$  limit however singles out the maximal non-commutative sphere solution by rendering the other extrema shorter lived; while making the dimension of the phase space in the non-abelian directions parametrically big with respect to that of the Cartan channels. This statement makes use of the details of the physics associated with the maximal non-commutative sphere solution; in particular, the facts that the number of unstable channels is independent of  $N$ , that the corresponding masses of the tachyons are also  $N$  independent, and that the instabilities arise at the longest wavelengths only.

Furthermore, it is interesting that the corresponding spherical D2 brane configuration is not unstable with respect to short wavelength perturbations; in contrast to the usual classical instabilities associated with bosonic membranes (see, for example, [25]). The phenomena we are studying may be generic with respect to couplings of non-commutative configurations to curved spaces. The  $M_{mn}\Phi^n\Phi^m$  term is a typical representative of many such couplings involving symmetrized products of the D0 brane matrix coordinates. This class of interactions arises in the DBI action due to the prescription introduced in [7, 17, 18] for replacing the spacetime dependence of background fields with the matrix coordinates of the D branes.

Given that the regime of interest is somewhat similar to the Matrix theory decoupling regime [20], and noting some of the similarities between our polarized configuration and

Matrix black holes [26, 27], it would be interesting to understand the relevance of all this to Matrix theory in curved spaces. In particular, extrema of actions describing an object as a probe in classical background fields necessarily contain qualitative information about the reverse effect, involving the back-reaction of the probes on the background fields.

Given that the potential energy is bottomless, one would also like to understand the relevance of decay through quantum mechanical tunneling. The corresponding dynamics would be naturally governed by  $\hbar$ , and its importance to the overall picture would be determined by the relative sizes between  $1/N$  and  $\hbar$ .

Finally, we may ask about explicit realizations of this effect of polarization by gravitational tidal forces. One system that is a candidate is the background geometry of near-extremal D6 branes. It can be shown that in this scenario we may expect the D0 branes to blow up into non-commutative D2 branes as they approach the finite area horizon. It may be instructive to understand the genericity of such an effect by exploring classes of background geometries.

## 7 Some details

In this section, we collect some of the details involved in analyzing the spectrum of eigenvalues of perturbations about the maximal non-commutative sphere solution. A similar analysis can be done for other extrema of the potential. Using (13) in (4), we obtain easily

$$\ddot{\mathbf{e}}^a = -2M'\mathbf{e}^a + \frac{M}{4} [\tau^b, [\tau^b, \mathbf{e}^a]] , \quad (27)$$

$$\ddot{\mathbf{e}}^i = -2M\mathbf{e}^i + \frac{M}{4} \left( [\tau^j, [\tau^j, \mathbf{e}^i]] + [\tau^j, [\mathbf{e}^j, \tau^i]] + [\mathbf{e}^j, [\tau^j, \tau^i]] \right) . \quad (28)$$

The perturbation modes can be written in a basis of harmonic modes as

$$\mathbf{e}^n = \sum_{l=1}^{N-1} \mathbf{e}_{i_1 \cdots i_l} \tau^{i_1 \cdots i_l} , \quad (29)$$

where [23, 22]

$$\tau^{i_1 \cdots i_l} \equiv \mathbf{Traceless} \left[ \mathbf{Sym} \left[ \prod_{j=1}^{j=l} \tau^{i_j} \right] \right] . \quad (30)$$

By **Sym** and **Traceless** we prescribe to symmetrize the product of Pauli matrices over  $i_1 \cdots i_l$ , and to project onto the subset traceless on any pair of indices. For fixed  $l$ , we have  $2l + 1$  independent traceless Hermitian matrices  $\tau^{i_1 \cdots i_l}$ . We note the following useful identity

$$\mathrm{Tr} \left[ \tau^{i_1 \cdots i_l} \tau^{j_1 \cdots j_m} \right] = 0 \quad \text{for } m \neq l ; \quad (31)$$

*i.e.* different harmonic modes decouple from each other. We also find the following commutation relations

$$[\tau^j, \tau^{i_1 \dots i_l}] = 2i \sum_a \varepsilon_{j i_a m} \tau_{i_a \rightarrow m}^{i_1 \dots m \dots i_l}, \quad (32)$$

$$[\tau^i, [\tau^j, \tau^{i_1 \dots i_l}]] = -4 \sum_{a \neq b} \varepsilon_{j i_a m} \varepsilon_{i i_b n} \tau_{i_a \rightarrow m; i_b \rightarrow n}^{i_1 \dots m \dots n \dots i_l} + 4l \delta_{ij} \tau^{i_1 \dots i_l} - 4 \sum_a \delta_{i_a i} \tau_{i_a \rightarrow a}^{i_1 \dots j \dots i_l}. \quad (33)$$

The notation is as follows:  $\tau_{i_a \rightarrow m}^{i_1 \dots m \dots i_l}$  means  $\tau^{i_1 \dots i_l}$  with the index  $i_a$  replaced by  $m$ . Substituting these relations in (27), we get

$$\ddot{\mathbf{e}}_{i_1 \dots i_l}^a = (Ml(l+1) - 2M') \mathbf{e}_{i_1 \dots i_l}^a. \quad (34)$$

We are then immediately led to the classical stability condition

$$M' \geq M. \quad (35)$$

In the three dimensional subspace where the D0 brane may expand, we get from (28)

$$\ddot{\mathbf{e}}_{i_1 \dots i_l}^i = V_{j; j_1 \dots j_l}^{i; i_1 \dots i_l} \mathbf{e}_{j_1 \dots j_l}^j, \quad (36)$$

with

$$V_{j; j_1 \dots j_l}^{i; i_1 \dots i_l} \equiv M \left( (l-2) \delta_{ij} \Delta + (l-2) \sum_a \delta_{i j_a} \Delta_{j_a \rightarrow j} + (l+1) \sum_a \delta_{j j_a} \Delta_{j_a \rightarrow i} \right). \quad (37)$$

We have defined

$$\Delta \equiv \delta_{i_1 j_1} \dots \delta_{i_l j_l}; \quad (38)$$

and  $\Delta_{j_a \rightarrow j}$  means  $\Delta$  with the corresponding substitution in one of the indices. Expression (37) is to be symmetrized in the indices  $\{i_1 \dots i_l\}$  and projected on the traceless subspace.

We then have an algorithm for computing the matrix (37). Diagonalizing it, we are led to a spectrum of eigenvalues for the perturbations modes. For a given  $N$ , we need to collect together all such eigenvalues with  $l < N$ <sup>5</sup>.

We have implemented this analysis using a computer. Diagonalizing the resulting matrices numerically, we obtained data about the spectrum. An analysis of the patterns in this spectrum inspired us to formulate the analytical description of the solution. One immediate and interesting observation is that all the eigenvalues appear to be integer multiples of  $M$  (with an exception to be noted below). Furthermore, a simple, yet non-trivial, pattern emerges. Some of the results were summarized in Section 3. Here, we describe a few more details.

For perturbations about the maximal non-commutative sphere solution, we obtain:

---

<sup>5</sup>In this harmonic basis, the perturbation matrix is block diagonal with respect to different harmonic mode sectors.

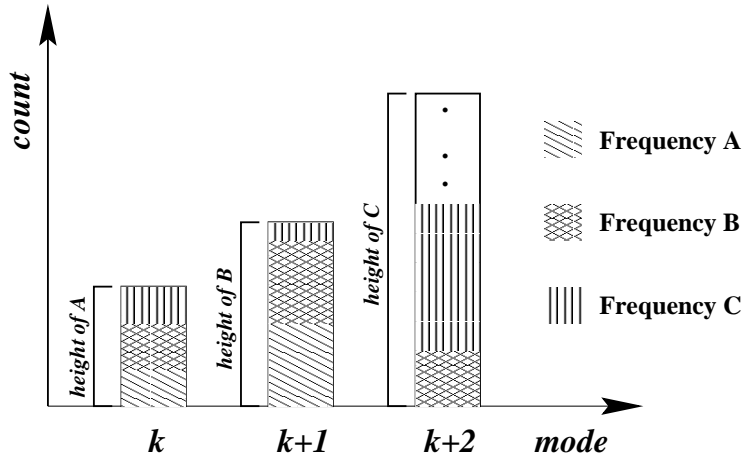


Figure 7: A schematic depiction of the distribution of stable perturbations across harmonic modes. The height of each bar reflects the number of stable eigenvalues in the corresponding harmonic mode. Each value of a positive frequency is represented by some shading pattern. The degeneracy of a given eigenvalue is proportional to the height of the corresponding shading pattern. These heights are in one to one correspondence with the total height of a bar with some fixed harmonic mode.

- Seven physical zero modes at harmonic mode number two.
- Five tachyonic modes at harmonic mode number one, with mass squared  $2M$ .
- Stable modes appear at all values of the harmonic numbers. The spectrum is interesting and is depicted in Figure 7. These modes can be labeled with a sequence of integers  $z = 2, 3, \dots$  such that the frequencies are given by

$$\omega_z^2 = -M(z^2 + z - 2) \text{ with degeneracy } d_z = 4z + 2 . \quad (39)$$

For a fixed value for  $z$ , the modes are distributed across a complex pattern of harmonic modes. Remarkably, the number of all stable modes appearing within a fixed harmonic mode  $m$ , with  $m \geq 3$ , is given by  $d_m$ . This pattern breaks down for dipole and quadrupole moments, but appears to be sustained for all higher ones. It may be an interesting mathematical problem to identify the mechanism responsible for this pattern of degeneracies.

For the  $n < N$  sphere solution, the spectrum is complex and, except for a few features, we cannot describe it analytically. We make the following observations:

- All frequencies are integer multiples of  $M$  only for *odd*  $N$ . Other details are also correlated with whether  $N$  is divisible by two.
- The number of unstable modes increases as  $N^2$ , for fixed  $n$ . The masses of these tachyonic modes are the same; we get  $\omega^2 = 2M$ .
- The number of stable modes increases as  $N$ .

For the maximal  $n = N$  disc solution, we find

- The number of physical zero modes is always equal to two.
- The number of unstable modes increases as  $2N - 2$ . The masses of these tachyonic modes appear as  $\omega^2 = 4M, 6M, \dots, 2NM$ .
- The number of stable modes increases as  $N^2$ .

**Acknowledgments:** I am particularly grateful to M. Spradlin and A. Volovich for drawing my attention to the problem of instability and for useful discussions. I also thank P. Argyres, T. Becher, M. Moriconi, H. Tye, and E. Yuzbashyan for many helpful discussions. This work was supported by NSF grant 9513717.

## References

- [1] N. Seiberg and E. Witten, “String theory and noncommutative geometry,” *JHEP* **09** (1999) 032, [hep-th/9908142](#).
- [2] R. Gopakumar, J. Maldacena, S. Minwalla, and A. Strominger, “S-duality and noncommutative gauge theory,” *JHEP* **06** (2000) 036, [hep-th/0005048](#).
- [3] R. Gopakumar, S. Minwalla, N. Seiberg, and A. Strominger, “OM theory in diverse dimensions,” [hep-th/0006062](#).
- [4] N. Seiberg, “A note on background independence in noncommutative gauge theories, Matrix model and tachyon condensation,” *JHEP* **09** (2000) 003, [hep-th/0008013](#).
- [5] J. McGreevy, L. Susskind, and N. Toumbas, “Invasion of the giant gravitons from anti-de Sitter space,” *JHEP* **06** (2000) 008, [hep-th/0003075](#).
- [6] S. R. Das, A. Jevicki, and S. D. Mathur, “Vibration modes of giant gravitons,” [hep-th/0009019](#).

- [7] R. C. Myers, “Dielectric-branes,” *JHEP* **12** (1999) 022, [hep-th/9910053](#).
- [8] S. R. Das, A. Jevicki, and S. D. Mathur, “Giant gravitons, BPS bounds and noncommutativity,” [hep-th/0008088](#).
- [9] S. R. Das, S. P. Trivedi, and S. Vaidya, “Magnetic moments of branes and giant gravitons,” [hep-th/0008203](#).
- [10] S. Mukhi and N. V. Suryanarayana, “Chern-simons terms on noncommutative branes,” *JHEP* **11** (2000) 006, [hep-th/0009101](#).
- [11] R. Tatar, “T duality and actions for noncommutative D-branes,” [hep-th/0011057](#).
- [12] Z. Guralnik and S. Ramgoolam, “On the polarization of unstable D0-branes into non-commutative odd spheres,” [hep-th/0101001](#).
- [13] L. Cornalba and R. Schiappa, “Nonassociative star product deformations for D-brane worldvolumes in curved backgrounds,” [hep-th/0101219](#).
- [14] I. Washington Taylor and M. V. Raamsdonk, “Multiple D0-branes in weakly curved backgrounds,” *Nucl. Phys.* **B558** (1999) 63–95, [hep-th/9904095](#).
- [15] V. Sahakian, “Transcribing spacetime data into matrices,” [hep-th/0010237](#).
- [16] I. Washington Taylor and M. V. Raamsdonk, “Multiple D0-branes in weakly curved backgrounds,” *Nucl. Phys.* **B558** (1999) 63–95, [hep-th/9904095](#).
- [17] M. R. Garousi and R. C. Myers, “World-volume interactions on D-branes,” *Nucl. Phys.* **B542** (1999) 73–88, [hep-th/9809100](#).
- [18] M. R. Garousi and R. C. Myers, “World-volume potentials on D-branes,” [hep-th/0010122](#).
- [19] S. F. Hassan and R. Minasian, “D-brane couplings, RR fields and Clifford multiplication,” [hep-th/0008149](#).
- [20] T. Banks, W. Fischler, S. H. Shenker, and L. Susskind, “M theory as a Matrix model: A conjecture,” *Phys. Rev.* **D55** (1997) 5112–5128, [hep-th/9610043](#).
- [21] F. K. Manasse and C. W. Misner, “Fermi normal coordinates and some basic concepts in differential geometry,” *Journal of Math. Phys.* **4** (1963) 735.

- [22] D. Kabat and I. Washington Taylor, “Spherical membranes in Matrix theory,” *Adv. Theor. Math. Phys.* **2** (1998) 181, [hep-th/9711078](#).
- [23] N. R. Constable, R. C. Myers, and O. Tafjord, “The noncommutative Bion core,” *Phys. Rev.* **D61** (2000) 106009, [hep-th/9911136](#).
- [24] M. R. Douglas, D. Kabat, P. Pouliot, and S. H. Shenker, “D-branes and short distances in string theory,” *Nucl. Phys.* **B485** (1997) 85–127, [hep-th/9608024](#).
- [25] Washington Taylor, “M(atrix) Theory: Matrix Quantum Mechanics as a Fundamental Theory,” [hep-th/0101126](#).
- [26] G. T. Horowitz and E. J. Martinec, “Comments on black holes in Matrix theory,” *Phys. Rev.* **D57** (1998) 4935–4941, [hep-th/9710217](#).
- [27] T. Banks, W. Fischler, I. R. Klebanov, and L. Susskind, “Schwarzschild black holes in Matrix theory. 2,” *J. High Energy Phys.* **01** (1998) 008, [hep-th/9711005](#).